ACS OMEGA

Open Access

http://pubs.acs.org/journal/acsodf

Article

Biocomposite Scaffolds Based on Chitosan Extraction from Shrimp Shell Waste for Cartilage Tissue Engineering Application

Chirapond Chonanant, Pongrung Chancharoen, Sirirat Kiatkulanusorn, Nongnuch Luangpon, Kultida Klarod, Pornprom Surakul, Niramon Thamwiriyasati, Sanita Singsanan, and Nipaporn Ngernyuang*

Cite This: *ACS Omega* 2024, 9, 39419−39429

Read Online

ACCESS | Metrics & More | Article Recommendations

ABSTRACT: Chitosan-based scaffolding possesses unique properties that make it highly suitable for tissue engineering applications. Chitosan is derived from deacetylating chitin, which is particularly abundant in the shells of crustaceans. This study aimed to extract chitosan from shrimp shell waste (*Macrobrachium rosenbergii*) and produce biocomposite scaffolds using the extracted chitosan for cartilage tissue engineering applications. Chitinous material from shrimp shell waste was deproteinized and deacetylated. The extracted chitosan was characterized and compared to commercial chitosan through various physicochemical analyses. The findings revealed that the extracted chitosan shares similar trends in the Fourier transform infrared spectroscopy spectrum, energy dispersive X-ray mapping, and X-ray diffraction pattern to commercial chitosan. Despite differences in the degree of deacetylation, these results underscore its comparable quality. The extracted chitosan was mixed with agarose, collagen, and gelatin to produce the blending biocomposite AG-CH-COL-GEL scaffold by freeze-drying method. Results showed AG-CH-COL-GEL scaffolds have a 3D interconnected porous structure with pore size 88−278 μm, high water uptake capacity (>90%), and degradation percentages in 21 days between 5.08% and 30.29%. Mechanical compression testing revealed that the elastic modulus of AG-CH-COL-GEL scaffolds ranged from 44.91 to 201.77 KPa. Moreover, AG-CH-COL-GEL scaffolds have shown significant potential in effectively inducing human chondrocyte proliferation and enhancing aggrecan gene expression. In conclusion, AG-CH-COL-GEL scaffolds emerge as promising candidates for cartilage tissue engineering with their optimal physical properties and excellent biocompatibility. This study highlights the potential of using waste-derived chitosan and opens new avenues for sustainable and effective tissue engineering solutions.

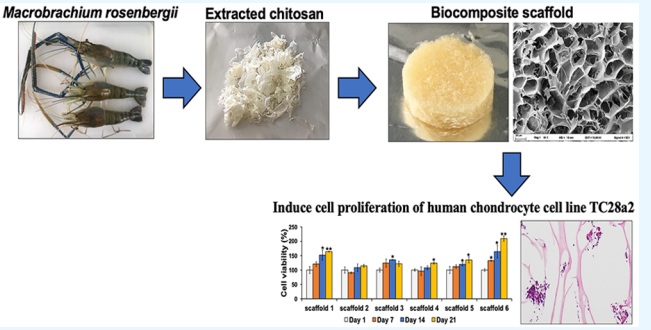

1. INTRODUCTION

Tissue engineering is an interdisciplinary field encompassing materials science, engineering, and biological sciences.[1] Tissue engineering aims to restore, maintain, or improve defective tissue functions or losses due to congenital disabilities, trauma, or surgery.[2] Tissue autografting and allografting are common approaches that have been used for replacing damaged or diseased tissue. Nevertheless, these approaches have several limitations, such as donor site morbidity and scarcity.[3] To eliminate the disadvantages of conventional clinical treatments, synthetic biocompatible scaffolds have been widely used in bone tissue engineering. The necessary ideal scaffold requirements include biocompatible, biodegradable, highly porous and interconnected, and mechanically reliable.[4] Numerous biomaterials have been already demonstrated to develop scaffolds for tissue engineering including polymeric biomaterials, bioceramics, metals, and carbon-based nanomaterials.[5−11]

One of the most widely used types of biomaterials in tissue engineering is natural polymers, which include agarose,[12−14] gelatin,[15,16] and collagen.[17,18] These polymers have been extensively investigated and proven to be suitable for creating 3D porous structures for *in vitro* models. They offer a microenvironment that closely mimics the extracellular matrix (ECM) found in the human body. Agarose has a good mechanical strength for the construction of scaffolds. The polysaccharide consisting of the agarose can form a hydrogel structure that has good mechanical strength and elasticity,[13,19] and it can also be processed using a freeze-drying

Received: March 27, 2024
Revised: July 27, 2024
Accepted: August 29, 2024
Published: September 10, 2024

technique.[20,21] Moreover, agarose scaffolds did not cause inflammatory responses.[22,23] Collagen consists of three polypeptide chains: glycine, proline, and hydroxyproline, arranged in a triple helix. The presence of Arg-Gly-Asp (RGD) sequences in collagen scaffold enhances cell attachment, increases cell proliferation,[17,18,24] and stimulates the chondrogenic differentiation of human bone marrow-derived mesenchymal stem cells.[18,25,26] Gelatin is often used in tissue culture for tissue engineering, because its structure is obtained via hydrolyzed collagen. Thus, gelatin shares structure as well as function with collagen.[27−29] In addition, the RGD sequence within the molecular structure of gelatin could support cell adhesion, proliferation, and differentiation.[30] These materials reveal suitable properties for tissue engineering in terms of biodegradability and biocompatibility. However, they have some limitations. Pure agarose scaffolds are unsuitable for cell adhesion due to their inert polymer nature.[12] Similarly, gelatin scaffolds face challenges with limited solubility in aqueous media and weak mechanical strength.[31,32] To address these limitations, natural polymers such as agarose and gelatin are often combined in mixtures. These blending materials improved mechanical properties, biological stability, and biocompatibility compared with single components.[33−36]

Chitosan has been extensively studied as a natural polymeric biomaterial, making it suitable for developing biomimetic scaffolds for tissue engineering and for the removal of heavy metals from wastewater.[37−40] Chitosan is a natural linear polysaccharide derived from the deacetylation of chitin that consists of 2-amino-2-deoxy-D-glycopyranose and 2-acetamide-2-desoxy-D-glycopyranose units linked together with β (1,4) glycosidic bonds.[41] Chitosan is considered highly biocompatible, biodegradable, bioactive, capable of promoting cell proliferation, cell adhesion, new bone tissue formation, and nontoxic *in vitro*.[42−44] Moreover, several studies have reported that chitosan-based scaffolds demonstrated excellent osteoconductivity *in vivo* in surgically created bone defects.[45,46] Significantly, chitosan is a facile material that can be used alone or combined with bioactive ceramics, synthetic polymers, and other natural polymers to create composite scaffolds with enhanced mechanical and biological performance.[47−49] Chitosan does not naturally occur in the environment. It is produced through the deacetylation of chitin, which is particularly abundant in crustacean shells, including those of shrimp, crab, and krill.[50] Shrimp shell waste has been reported as the most remarkable and good source of chitosan.[51]

The freshwater giant prawn (*Macrobrachium rosenbergii* De Man) is recognized as one of the most economically important indigenous species with high demand in both domestic and export markets. Shrimps are typically sold headless and often the outer shell is peeled off, thus the shrimp head, shell, and tail are generated as waste. This results in the generation of a large amount of biowaste globally.[52] Chitin and chitosan are versatile, environmentally friendly, and modern materials isolated from shrimp biowaste. Thus, the extraction and depolymerization of chitin and chitosan could be a waste disposal alternative and product recovery method from shrimp biowaste.[53]

Therefore, this study aims to extract chitosan from shrimp (*M. rosenbergii*) shell waste and demonstrate its application in cartilage tissue engineering. The extracted chitosan was then used as a natural material to develop a biocomposite scaffold (agarose-extracted chitosan-collagen-gelatin, AG-CH-COL-GEL) by using freeze-drying method. The AG-CH-COL-GEL scaffolds exhibited a three-dimensional (3D) interconnected porous structure with pore sizes ranging from 88 to 278 μm, which is crucial for nutrient and waste exchange in tissue engineering. These scaffolds exhibit high water uptake capacity and excellent mechanical properties. They are also compatible with chondrocytes and stimulate the expression of the aggrecan gene.

2. MATERIALS AND METHODS

2.1. Materials. Chitosan, collagen, and gelatin were purchased from Himedia (Mumbai, India). Agarose was purchased from Sisco Research Laboratories (Mumbai, India). NaOH and HCl were purchased from Merck. Human chondrocyte cell line TC28a2, MTT reagents (3-(4,5-dimethylthiazol-2-yl)-2,5-diphenyltetrazolium bromide), glutaraldehyde solution, acetic acid, and formaldehyde were purchased from Sigma-Aldrich (St Louis, MO, USA). Dulbecco's modified Eagle's medium with high glucose (DMEM-HG) and penicillin/streptomycin (P/S) was supplied from Gibco (Grand Island, NY, United States). Fetal bovine serum (FBS) was purchased from HyClone (Cramlington, UK).

2.2. Extraction of Chitosan from Shrimp Shell Waste. Chitosan extraction in this study was modified by Benjakul S et al.[54] The process of chitosan extraction is divided into three major steps including the demineralization of shrimp shells, chitin processing (deproteinization), and chitosan processing (deacetylation).[55] The *M. rosenbergii* shrimp shell waste was collected and washed several times with tap water. After drying, shrimp shells were ground into smaller pieces by using a grinder. The smaller pieces of shrimp shell are demineralized with 1.25 N HCl (1:10 w/v) at room temperature for 1 h. After the incubation period, the shells became quite squashy and were rinsed with deionized water (DI) to remove the acid and calcium carbonate. After demineralization, the demineralized shells were deproteinized by treating them with 10% NaOH (1:10 w/v) at 100 °C for 1 h. After processing, the residue was washed with DI to remove NaOH. The resulting product is called chitin. Deacetylation is the process of converting chitin to chitosan by removing the acetyl group. The chitin was treated with 50% NaOH (1:10 w/v) at 100 °C for 30 min, followed by intensive washing with DI to remove NaOH residues. After the mixture was dried, the final product recovered was chitosan.

2.3. Degree of Deacetylation (DD) for Chitosan. The DD values of chitosan were determined using an acid−base conductometric titration method. Briefly, 0.1 g of chitosan was dissolved in 30 mL of 0.1 N HCl aqueous solution at room temperature, and 3 drops of methyl orange were added. The chitosan solution was then titrated with 0.1 N NaOH until the red chitosan solution turned orange. The DD value of the chitosan sample was calculated using the following equation:

$$\mathrm{DD}\% = \frac{(V_1 - V_2) \times 16}{V_1 \times 9.94 \times x} \times 100$$

where x represents the weight of dried chitosan; V_1 is the volume of chitosan solution prepared in 0.1 N HCl (in mL); V_2 is the volume of 0.1 N NaOH (in mL); 9.94 is the theoretical percentage of amino group content in chitosan; and 16 is the gram equivalent weight of the amino group.[56]

2.4. Physicochemical Characterization of Extracted Chitosan. Fourier transform infrared spectroscopy (FTIR)

https://doi.org/10.1021/acsomega.4c02910
ACS Omega 2024, 9, 39419−39429

was employed to identify the functional groups in both standard chitosan and extracted chitosan. The analysis was conducted using Nicolet iS50 FTIR spectrometers from Thermo Fisher Scientific. Each spectrum was recorded as the average of 64 scans with a resolution of 4 cm^{-1} over the wavenumber range of 400−4000 cm^{-1}. An energy dispersive X-ray spectrometer (EDS) was performed to obtain morphological information on the membrane surface using the JSM7800F (JSM7800F; JEOL, Tokyo, Japan). The X-ray diffraction (XRD) patterns were analyzed by using a D8 ADVANCE Bruker AXS diffractometer (Bruker, Karlsruhe, Germany). The crystalline structure was examined at a voltage of 40 kV and a current of 40 mA with Cu radiation (1.5406 Å) over a 2θ range of 10−90° with a scan speed of 0.02° per step.

2.5. Preparation of Biocomposite Agarose-Extracted Chitosan-Collagen-Gelatin (AG-CH-COL-GEL) Scaffolds. The biocomposite scaffolds were produced according to the instructions reported by Tripathi et al.[57] with modifications. Briefly, agarose (final concentration, 3% w/v) was dissolved in DI by boiling until a clear, transparent solution was obtained. The extracted chitosan at concentrations of 1% w/v was prepared by dissolving in 1% aqueous acetic acid solution. Collagen (final concentration 0.5%, 1%, and 3% w/v) was dissolved in DI. Gelatin was dissolved in DI with concentrations of 0.5% and 1% w/v. To optimize the scaffold properties, the different ratios of agarose, chitosan, and gelatin were listed in Table 1. The biocomposite solution containing

Table 1. Formulation of AG-CH-COL-GEL Composite Scaffolds

Scaffold	Agarose (AG)	Chitosan (CH)	Collagen (COL)	Gelatin (GEL)
1	3%	1%	0.5%	0.5%
2	3%	1%	0.5%	1%
3	3%	1%	1%	0.5%
4	3%	1%	1%	1%
5	3%	1%	3%	0.5%
6	3%	1%	3%	1%

agarose, chitosan, and gelatin was cross-linked by using 0.5 mL of glutaraldehyde solution (0.2% v/v) and incubated at −80 °C for 24 h. Then, the solution mixture was subsequently freeze-dried under a vacuum at −100 °C for 48 h (Martin Christ, Germany). The biocomposite AG-CH-COL-GEL scaffold was dried at room temperature and cut into discs (thickness: 0.5 cm and diameter: 1.5 cm) for further studies.

2.6. Scanning Electron Microscopy (SEM). The surface morphology of the freeze-dried scaffolds was examined by using a Hitachi SU8000 scanning electron microscope (HI-0210−0005, Hitachi High-technologies; Düsseldorf, Germany) at an accelerating voltage of 10 kV. A small piece of the scaffold was fixed onto an aluminum stub using double-sided carbon tape and then gold-coated before its surface was observed with SEM imaging. The pore size of the scaffold was determined by analyzing SEM observation images with ImageJ software.

2.7. Water Uptake Ability. The water uptake measurement was performed by immersing the biocomposite scaffolds in a phosphate buffered saline (PBS) solution with a pH of 7.4. Briefly, the scaffold was cut into discs with a thickness of 0.5 cm and a diameter of 1.5 cm. The dry scaffold was weighed (W_{dry}) and immersed in 1× PBS for 1 h. After the incubation period, the weight of the swollen scaffolds (W_{wet}) was recorded following the removal of the excess surface PBS with filter paper. The water uptake percentage of the scaffolds was calculated using the following formula.[41,42] The reported water uptake was determined by averaging the values obtained from three samples.

$$\text{Water uptake ability (\%)} = \frac{W_{wet} - W_{dry}}{W_{dry}} \times 100$$

2.8. *In Vitro* Degradation. The degradation of the AG-CH-COL-GEL scaffold was calculated by weight loss measurements. The scaffolds were cut into discs with a thickness of 0.5 cm and a diameter of 1.5 cm, weighed (W_1), and then immersed in a sterile 1× PBS solution (pH 7.4) at 37 °C for 3 weeks. At the specified time points, 1 week, 2 weeks, and 3 weeks of incubation, triplicated samples were removed, dried at 80 °C in a hot air oven, and then weighed (W_2). The degree of degradation was determined by the change in dry weight using the following formula.[58]

$$\text{Degradation rate (\%)} = \frac{W_1 - W_2}{W_1} \times 100$$

2.9. Mechanical Analysis. The mechanical properties of the six scaffolds were assessed using a Materials Testing Machine (Zwick/Roell, Proline Z010, Germany). Three samples from each group of the scaffold were tested to measure the compressive modulus, using a crosshead speed of 0.5 mm/min with a loading weight of 1 kN. The stress−strain data for all groups were then analyzed, and the compressive modulus was calculated based on the resulting stress−strain curves.

2.10. Cell Culture. The normal human chondrocyte cell line TC28a2, passages 3−4, was used as a model for studying cartilage tissue engineering. This cell line was obtained from Sigma-Aldrich. The cells were cultured in DMEM-HG supplemented with 1% P/S and 10% FBS. The cells were cultured in a humidified incubator at 37 °C with 5% CO_2.

2.11. Cell Culture on AG-CH-COL-GEL Scaffolds. The scaffold with a thickness of 0.5 cm and a diameter of 1.5 cm was plated into a cell culture disc and immersed in 2% NaOH to neutralize the residual acid in the scaffold. The scaffold was washed five times with DI. Both sides of the scaffold were sterilized using 70% ethanol followed by exposure under ultraviolet irradiation in a biological safety cabinet for 30 min before further study. TC28a2 cells (1×10^6 cells/20 μL) were dropped slowly onto the top surface of each scaffold. To allow the cells to adhere to the scaffold, cell seeding on the scaffold was then cultured in a CO_2 incubator for 2 h. Then the cells/scaffold constructs were submerged with 5 mL of DMEM-HG supplemented with 1% P/S and 10% FBS and cultured at 37 °C in a humidified atmosphere containing 5% CO_2. The cellular scaffold was harvested at 1, 7, 14, and 21 days for further study. The cell culture medium was replaced every 3 days.

2.12. Cell Viability Assay. To determine the viability and proliferation of the normal human chondrocyte cell line TC28a2 in the AG-CH-COL-GEL scaffold, an MTT assay was carried out. The cell/scaffold constructs cultured for 1, 7, 14, and 21 days were harvested. After the end of each time point, the formazan crystal formed in the cell was solubilized by isopropanol. The supernatant was transferred to a new 96-well plate to avoid interference from scaffold absorption, and cellular absorbance was measured at 570 nm using a plate

https://doi.org/10.1021/acsomega.4c02910
ACS Omega 2024, 9, 39419−39429

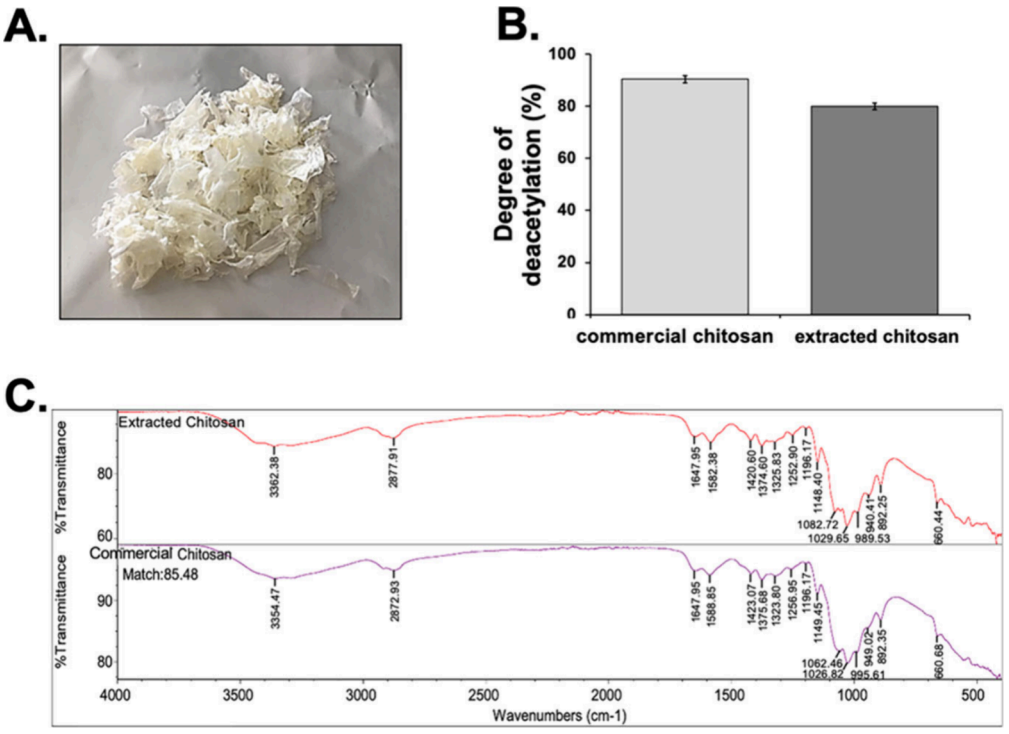

Figure 1. Chitosan was extracted from shrimp shell waste in this study. (A) Image of extracted chitosan. (B) The representative bar graph of DD values shows the average results from triplicate samples of both commercial chitosan and chitosan extracted from shrimp shell waste. (C) The FTIR spectra of chitosan from shrimp shell waste were compared to those of commercial chitosan.

reader spectrophotometer (VersaMax). The data were obtained from three independent experiments. The percentage of viable cells was calculated by normalizing to the 1-day control.

2.13. Hematoxylin and Eosin (H&E Stain). The cell/scaffold constructs cultured for 1, 7, 14, and 21 days were harvested. At each time point, the constructs were washed three times with PBS, fixed in 4% phosphate-buffered paraformaldehyde for 24 h, dehydrated through a graded series of ethanol, embedded in paraffin wax, and then sectioned into 10 μm thick slices. The tissue sections for histological analysis were soaked in xylene for 5 min for removed paraffin, 90%, 80%, and 70% ethanol were used as rehydrated reagents. After the rehydrated process, the sections were stained with hematoxylin and eosin. The sample was dehydrated again and mounted with coverslip slides using permount. All types of scaffolds also observed the microstructure by H&E staining.

2.14. Reverse Transcription Polymerase Chain Reaction (RT-PCR). Total RNA was extracted from induced cells on days 7, 14, and 21 using the RNeasy mini kit (Qiagen, Germany) according to the manufacturer's instructions. The first strand complementary DNA (cDNA) was synthesized by reverse transcription with oligo d(T) primers by using the SuperScript III reverse transcriptase kit. RT-PCR was performed to detect the expression level of chondrocyte marker genes including *SRY-Box Transcription Factor 9* (*SOX9*), *collagen type II* (*Col II*), *aggrecan* (*AGC*), and *glyceraldehyde-3-phosphate dehydrogenase* (*GAPDH*: reference gene) using a Toptaq Master Mix Kit (Qiagen, Hilden, Germany). The PCR reaction of the above genes was conducted using a Thermal Cycler (Corbett Life Science, Australia) with the primers from our previous study.[59] Triple reactions were performed for all of the genes. Finally, the amplified product was separated by 2% agarose gel electrophoresis, stained with Cybergold (Sigma-Aldrich), and visualized by using a UV Tran illuminator.

2.15. Statistical Analysis. All experiments were conducted in triplicate, and data were represented as means ± standard deviation (SD). All statistical analyses were performed using GraphPad Prism (v.8.0.2) by one-way ANOVA with Tukey's multiple comparison tests to check the significant difference among the samples. The *p*-value of less than 0.05 was considered statistically significant.

3. RESULTS AND DISCUSSION

3.1. Characteristics of Extracted Chitosan. The characteristics of chitosan extracted from the *M. rosenbergii* shell showed a bright off-white color (Figure 1A). This result was consistent with Tamzi et al.[60] The quality and bioactive properties of chitosan significantly depend on DD, which is defined as the mole fraction of deacetylated units in the polymer chain. Therefore, the determination of DD has been the most important parameter in studying chitosan preparations.[61] The DD obtained from shrimp shell waste in this study was 79.95 ± 1.36% compared to commercial standard chitosan 90.42 ± 1.42% as in Figure 1B. Our results were consistent with previous studies that the extracted chitosan usually obtained a DD in the range of 62−79% and the commercial chitosan samples had an average DD of 70−90%, therefore the chitosan produced from shrimp shell waste in this study is of acceptable quality.[62−64] The DD values can be different due to different raw materials and the method of extraction processes.[65,66] The deacetylation process involves removing acetyl groups from the chitin molecular chain through hydrolysis with concentrated NaOH, resulting in the formation of an amino group ($-NH_2$). The properties of chitosan are closely related to the high degree of chemically reactive amino

https://doi.org/10.1021/acsomega.4c02910
ACS Omega 2024, 9, 39419−39429

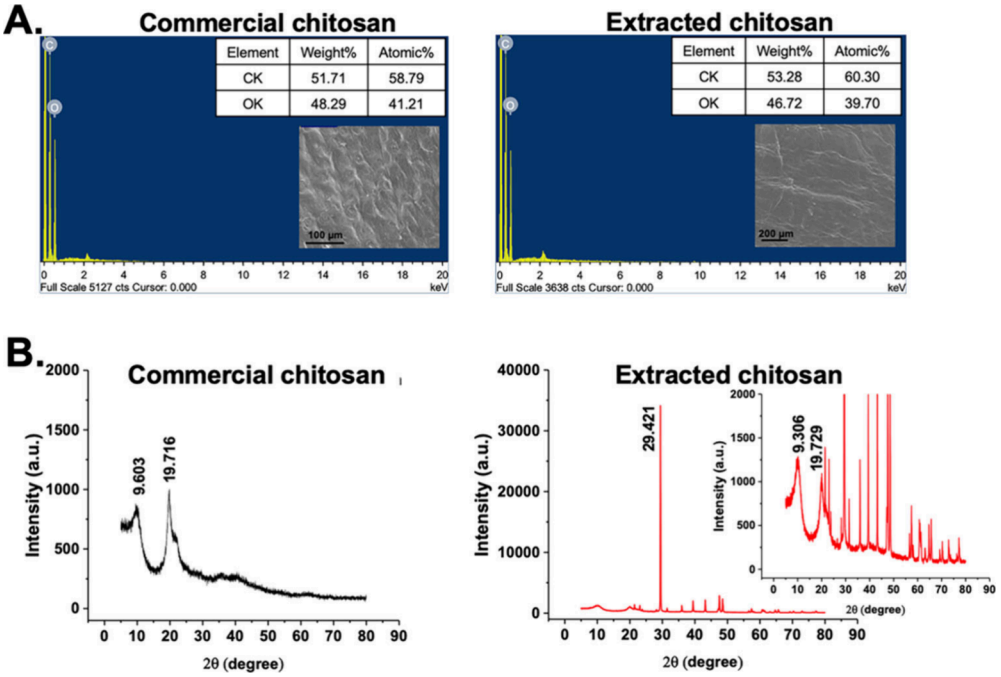

Figure 2. Extract chitosan was characterized using (A) SEM/EDX and (B) XRD analysis. The SEM, EDX, and XRD analysis showed that both commercial and extracted chitosan exhibited similar patterns. This indicates that the chitosan extracted from shrimp shell waste closely resembles commercial chitosan in terms of composition and structure.

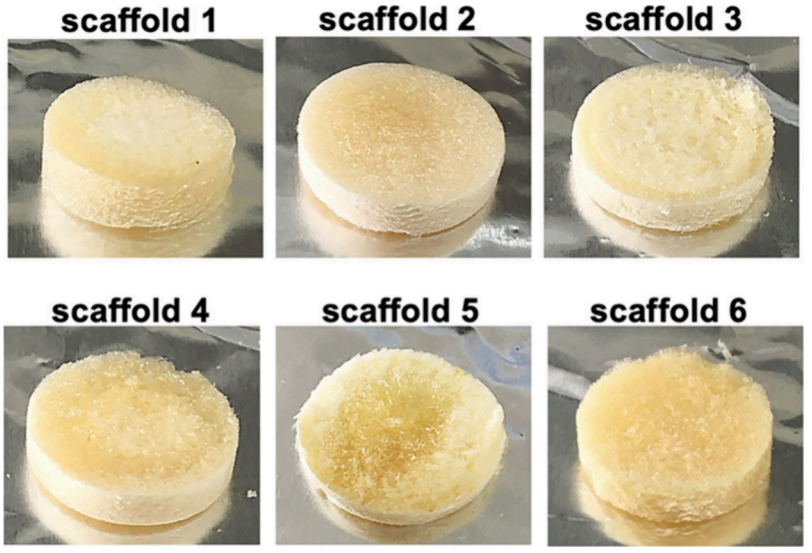

Figure 3. Photographic image of AG-CH-COL-GEL composite scaffolds shows all six types of scaffolds synthesized in 3D porous structures using the freeze-drying technique, resulting in a sponge-like structure.

groups present.[67] FTIR spectra were used to detect functional groups and chemical structures of extracted chitosan from shrimp shell waste, as shown in Figure 1C. A peak at 3362.38 cm^{-1} corresponds to the −OH stretching vibrations of water and hydroxyls, as well as the NH_2 stretching vibrations of free amino groups. The peak observed at 2877.91 cm^{-1} corresponds to an asymmetric stretching of CH_2 in chitosan. The amide frequencies, corresponding to the −C−O bond stretching of the remaining acetamido groups, are observed at 1647.95 and 1582.33 cm^{-1}. The band at 1582.33 cm^{-1} has a greater intensity than the one at 1647.95 cm^{-1}, indicating effective deacetylation.[68] The peak at 1420.60 cm^{-1} is assigned to $-NH_2$ deformation, while further bending vibrations are observed at 1374.60 cm^{-1} for the C−C−H symmetric bending vibration in the alcohol. Stretching vibrations are observed at 1148.40 cm^{-1} for the C−N stretching vibration and 1082.72 and 1029.65 cm^{-1} for the −CO stretching vibration of the alcohol groups. The observation in this spectrum analysis is similar to what was observed by Muñoz et al.[69] and Hassan.[70] The presence of a band stretching pattern in the extracted chitosan that corresponds to the band stretching of commercial standard chitosan indicates that the extracted material is indeed chitosan.

EDX is an X-ray technique used to identify the elemental composition of a material. All EDX spectrum analyses for commercial standard chitosan and extracted chitosan are

https://doi.org/10.1021/acsomega.4c02910
ACS Omega 2024, 9, 39419−39429

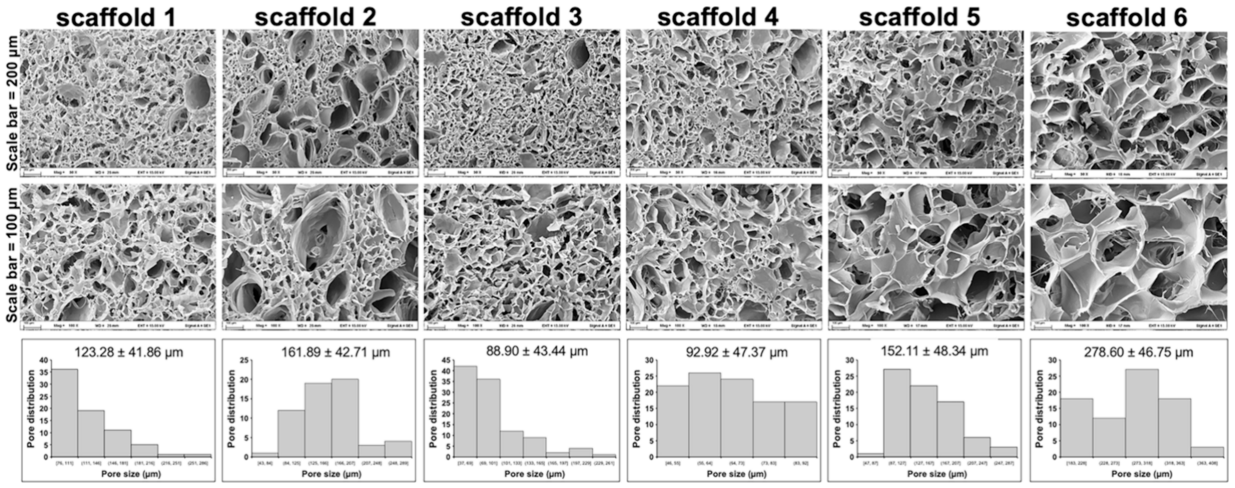

Figure 4. SEM images of the AG-CH-COL-GEL composite scaffolds in different conditions. (A) Representative SEM image of the scaffolds showing a 3D geometry with spherical pore units arranged in a honeycomb pattern. (Upper row) The scale bar equals 200 μm. (Middle row) The scale bar equals 100 μm. (Bottom row) The pore distribution in the scaffolds.

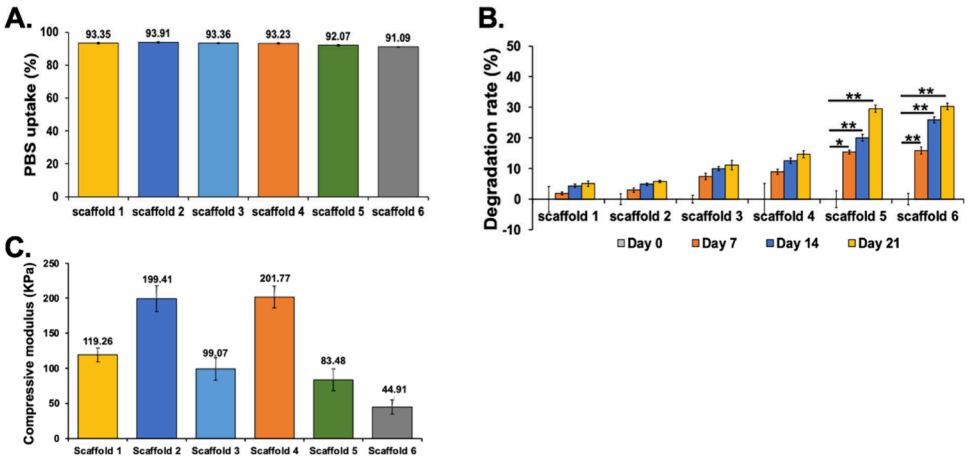

Figure 5. Water absorption capability, degradation rate, and compressive property of the AG-CH-COL-GEL composite scaffolds were assessed as follows. (A) The water absorption capability of the scaffold composite. (B) The degree of degradation of the scaffolds. (C) The compressive properties of the AG-CH-COL-GEL composite scaffolds. The data were presented as mean ± SD. Each error bar represents the SD from triplicate experiments, analyzed using One-Way ANOVA. The $^{*}p < 0.05$ and $^{**}p < 0.01$ indicate statistically significant differences when compared to day 0.

shown in Figure 2A. From the results, it could be observed that there are peaks for elements like carbon (C) and oxygen (O) with different intensities. In the extracted chitosan, the weight of C and O levels was 53.28% and 46.72%, respectively. Similarly, the percentages of C and O observed for standard chitosan were 51.71% and 48.29%, respectively. For assessing the purity of the product, the percentage of nitrogen (N) is crucial as it serves as a key indicator. Our extracted chitosan was not observed in the N value, indicating that no protein remnants in the samples. This result demonstrates the effectiveness of diluted acid in removing all protein and minerals from the shrimp shells.[71] Therefore, it can be assumed that the chitosan extracted from shrimp shell waste in this study is very similar to commercial chitosan.

The crystalline nature and phase formation of the standard chitosan and extracted chitosan were determined using XRD analysis. X-ray diffraction studies of standard chitosan exhibit vast peaks at $2\theta = 9.603°$ and $2\theta = 19.716°$ corresponding to crystalline reflections of 020 and 110, respectively (Figure 2B). By contrast, 34 strong peaks were observed in the extracted chitosan, among which the strongest peak was observed at $2\theta = 29.421°$ (intensity 29161.8). The extracted chitosan still displayed crystalline reflections of 020 and 110 corresponding to 2θ of 9.306° and 19.729°, similar to standard chitosan. These diffraction angles at 2θ of 20° and 30° are the characteristic regions of chitosan phases and calcite or calcium phosphate family, respectively.[72] This result was consistent with the α-crystalline structures of chitosan prepared from swimming crab shells.[73] Additionally, the XRD diffraction patterns of chitosan have been reported to have a peak broader and less intense compared to those of chitin, which is due to the structural changes that occur during the deacetylation process. Our extracted chitosan exhibits several peaks in its XRD pattern, unlike commercial chitosan, which is likely due to its lower DD (79.95 ± 1.36). These results are in accordance with Zhang et al.[74]

3.2. Characteristics of Synthesized AG-CH-COL-GEL Scaffolds. The fabricated scaffolds were pale yellow and had a 3D structure like spongy, as shown in Figure 3. SEM was used to investigate the surface morphology of AG-CH-COL-GEL scaffolds displayed in Figure 4. All scaffolds displayed interconnected open pores with irregular and polygonal pore

https://doi.org/10.1021/acsomega.4c02910
ACS Omega 2024, 9, 39419−39429

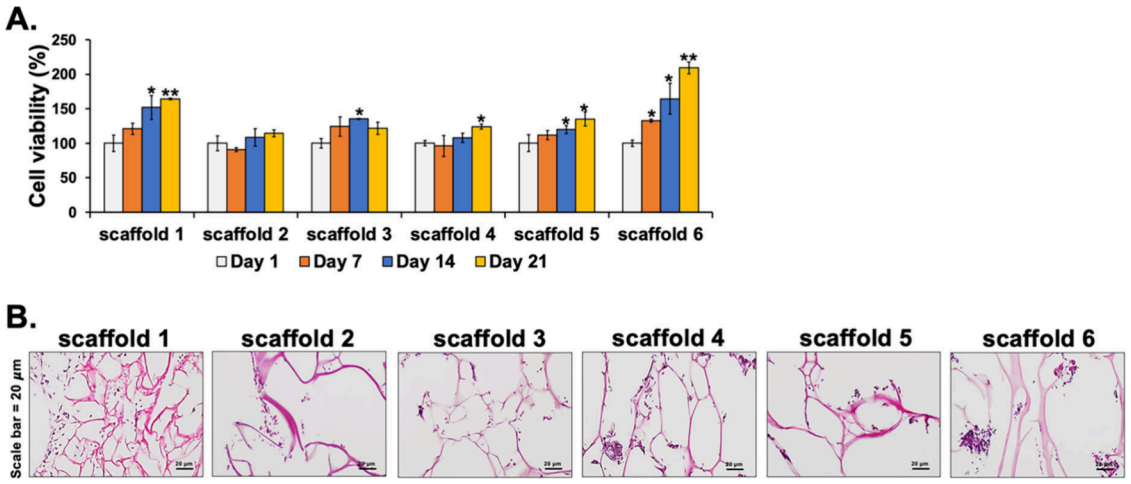

Figure 6. Biocompatibility analysis of the AG-CH-COL-GEL composite scaffolds. (A) The cell viability of chondrocytes on scaffolds 1, 7, 14, and 21 days was evaluated by an MTT assay. The data were presented as mean ± SD. Each error bar represents the SD from triplicate experiments, analyzed using One-Way ANOVA. *$p < 0.05$ and **$p < 0.01$ indicate statistically significant differences when compared to day 1. (B) Representative images from histological sections of the chondrocyte-seeded constructs after 21 days of culture incubation showed the scaffold pore geometry in all images. The sections were stained with hematoxylin and eosin, with cell nuclei appearing purple and the cell cytoplasm stained pink. The scale bar equals 20 μm in all images.

structures, with an average pore size of around 88−278 μm. The average pore size of scaffold 6 is larger than that of the other scaffold. Our findings are in agreement with previous studies, which suggest that the average pore size in the scaffold increased when higher concentrations of gelatin were used.[75]

An important factor for scaffolds used in tissue engineering is water uptake.[76] This property affects the transport of water and nutrients into the scaffold, thereby promoting cell proliferation and differentiation.[77] The volume of water that was absorbed by the scaffold was defined by swelling them in PBS (pH 7.4) at 37 °C for 1 h. The water uptake capacity is presented in Figure 5A. According to the results, scaffold 2 showed the maximum water uptake ability, while scaffold 6 showed the lowest water uptake capacity. The water uptake potential decreases as the hydrophobicity increases because the number of hydrophilic groups decreases.[78] In this study, the water uptake potential of the composite scaffold decreases after adding collagen and gelatin, likely due to the interplay of the hydrophobic and hydrophilic interactions within these molecules. Collagen and gelatin contain hydrophilic groups, such as amino and hydroxyl groups, which can interact with the hydrophilic sites on chitosan. This interaction can potentially block the hydrophilic sites on chitosan from bonding with water molecules, thereby decreasing the scaffold's overall water uptake potential.[79] However, statistical analysis showed no significant difference among all AG-CH-COL-GEL scaffolds ($p > 0.05$). Additionally, all AG-CH-COL-GEL scaffolds exhibited high water uptake capacity, reaching up to 90%.

Biodegradability is an essential property for designing scaffolds in tissue engineering applications. The scaffolds should ideally degrade through a controlled mechanism and be absorbed by the surrounding tissues without the need for surgical removal.[80] The biodegradation behavior of the AG-CH-COL-GEL scaffolds was assessed by incubating them in PBS at 37 °C for 7, 14, and 21 days, as shown in Figure 5B. The results showed that the biodegradation rate increased with a higher concentration of collagen used in scaffold fabrication.[81] Notably, scaffolds 1 and 2 exhibited minimal mass loss by 21 days (approximately 6% of their weight) due to the low concentration of collagen incorporated. In contrast, the weight of scaffold 5 and scaffold 6 had significantly decreased by 15% after 7 days and further decreased to 30% ($p < 0.05$) by 21 days, attributed to the high concentration of collagen used. In this study, we found the highest degradation rate in scaffold 6 which consists of higher collagen and gelatin concentration. The biodegradation rate enhanced in scaffold 6 might be due to the addition of components that are more readily biodegradable such as collagen and gelatin (denatured form of collagen), which can enhance the overall biodegradation rate of the scaffold. Additionally, it must be acknowledged that the scaffolds with larger pore sizes degraded faster than those with smaller pore sizes.[82] Thus, scaffold 6 is more easily broken down by biological processes than the other scaffold. In addition, the fact that scaffold 6 has the largest pore size, around 278 μm, results in a greater surface area exposed to water, which may influence the degradation rate of the scaffold.

The mechanical properties of the scaffold are important factors in designing scaffolds that will be used in cartilage tissue engineering. The compressive properties of AG-CH-COL-GEL scaffolds are seen in Figure 5C. It was found that the compressive modulus of scaffolds 1−6 were 119.26 ± 9.94, 199.41 ± 18.29, 99.07 ± 16.02, 201.77 ± 15.26, 83.48 ± 15.52, and 44.91 ± 10.02 KPa, respectively. Notably, the increase in mechanical properties of scaffolds 1−5 in comparison with scaffold 6 could also be attributed to the decrease in the pore size.[83,84]

3.3. Biocompatibility of the AG-CH-COL-GEL Scaffolds on Human Chondrocyte Cells. An ideal tissue engineering scaffold should not induce cell cytotoxicity, which can be evaluated through *in vitro* MTT cytotoxic tests. Human chondrocyte cells were cultured on AG-CH-COL-GEL scaffolds for up to 21 days. The cell viability of each AG-CH-COL-GEL scaffold in contact with chondrocyte cells at different time points as quantified by the MTT assay is presented in Figure 6A. The cell viability continued to increase during the culture period, indicating that all prepared AG-CH-

https://doi.org/10.1021/acsomega.4c02910
ACS Omega 2024, 9, 39419−39429

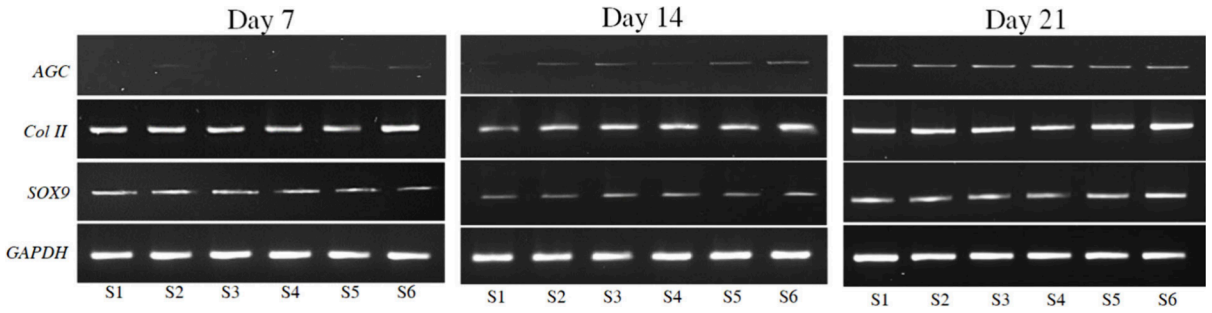

Figure 7. Semiquantitative analysis of chondrocyte marker genes: *SOX9*, *Col II*, and *AGC* at 7, 14, and 21 days of culture chondrocyte on the biocomposite scaffold. The study on cartilage gene expression showed that while *Col II* and *SOX9* expression levels were similar among cells cultured on six scaffolds, the *AGC* gene expression progressively increased from days 7 to 21.

COL-GEL scaffolds have no cytotoxicity and good biocompatibility. The cell viability of AG-CH-COL-GEL scaffold 6 after 21 days was significantly higher compared to other groups, indicating that the pore size of 278.60 ± 46.75 μm is appropriate for the chondrocyte proliferation. This result is in line with a previous study where the chondrocytes exhibited preferential proliferation and extracellular matrix production for scaffolds with pore sizes between 250 and 500 μm.[27] Pore size on the porous scaffold also plays an important role in the proliferation and differentiation of chondrocyte cells.[85] Several studies demonstrate the increasing cell proliferation found in scaffold constructs, with increasing scaffold pore size.[27,86] These results may be attributed to the complexity of factors in a 3D culture, which can influence cell penetration, distribution, cell migration, and nutrient flow. However, some studies have demonstrated that the chondrocyte phenotype improved in collagen matrices containing smaller pores.[87,88]

Moreover, the cross-sectional views and H&E staining of the AG-CH-COL-GEL scaffolds at 21 days of culture were selected for comparison. Figure 6B shows that cells had grown in the pores of the AG-CH-COL-GEL scaffold. The overall purple contrast of scaffold 6 is darker than other scaffolds, indicating that scaffold 6 is more suitable as a cartilage scaffold for chondrocytes. In addition, scaffold 6 was degraded by 30% after 21 days of exposure, which is very promising since the appropriate degradation rate can be achieved for the proliferation of chondrocytes in a cartilage implant.

The study of cartilage gene expression revealed that the expression levels of *Col II* and *SOX9* were similar across all scaffolds (Figure 7). However, the expression level of the *AGC* gene increased progressively from day 7 to day 21. Specifically, *AGC* expression was detected earlier (on day 14) in cells cultured on scaffolds 2, 3, 5, and 6 compared to scaffolds 1 and 4, where *AGC* expression was observed on day 21. This indicates that scaffolds 2, 3, 5, and 6 are more effective at promoting *AGC* gene expression. The scaffolds ranging from 152 to 278 μm (scaffolds 2, 5, and 6) likely create an optimal environment for cell growth, thereby enhancing aggrecan gene expression. Interestingly, scaffold 3, with a pore size of around 88 μm, also promotes aggrecan gene expression from day 14. This indicates that multiple factors might influence the effectiveness of cell cultivation on scaffolds, necessitating further study.

4. CONCLUSION

In this study, chitosan was extracted from *M. rosenbergii* shrimp shell waste and then applied to produce biocomposite scaffolds in cartilage tissue engineering applications. The extracted chitosan was characterized in terms of physicochemical properties. The results showed that the extracted chitosan had similar trends in the FTIR spectrum, EDX, and XRD pattern compared to commercial chitosan indicating that extracted chitosan has comparable properties to commercial chitosan. The blending biocomposite AG-CH-COL-GEL scaffold based on extracted chitosan was fabricated by freeze-drying method. The AG-CH-COL-GEL scaffolds exhibit suitable porosity and great physicochemical properties for cartilage tissue engineering applications. The *in vitro* cytocompatibility was screened using human chondrocyte cell line TC28a2 showing that AG-CH-COL-GEL scaffolds were noncytotoxic and were able to enhance cell proliferation for the time of culture. Therefore, the AG-CH-COL-GEL scaffolds, especially scaffold 6 may be promising biocomposite scaffold structures for cartilage tissue engineering applications. However, a limitation of this study is that we did not produce the AG-CH-COL-GEL scaffolds using commercial chitosan or test different concentrations of extracted chitosan. Furthermore, future studies should include cell migration studies and animal models to evaluate the long-term biological performance, stability of the scaffolds, and efficacy outcomes.

AUTHOR INFORMATION

Corresponding Author

Nipaporn Ngernyuang − *Thammasat University Research Unit in Biomedical Science and Chulabhorn International College of Medicine, Thammasat University, Pathum Thani 12120, Thailand;* orcid.org/0000-0002-8586-6115; Email: nngernyuang@gmail.com

Authors

Chirapond Chonanant − *Department of Medical Technology, Faculty of Allied Health Science, Burapha University, Chonburi 20131, Thailand*

Pongrung Chancharoen − *Department of Medical Sciences, Faculty of Allied Health Sciences, Burapha University, Chonburi 20131, Thailand*

Sirirat Kiatkulanusorn − *Department of Physical Therapy, Faculty of Allied Health Sciences, Burapha University, Chonburi 20131, Thailand*

Nongnuch Luangpon − *Department of Physical Therapy, Faculty of Allied Health Sciences, Burapha University, Chonburi 20131, Thailand*

Kultida Klarod − *Department of Physical Therapy, Faculty of Allied Health Sciences, Burapha University, Chonburi 20131, Thailand*

https://doi.org/10.1021/acsomega.4c02910
ACS Omega 2024, 9, 39419−39429

Pornprom Surakul − *Department of Physical Therapy, Faculty of Allied Health Sciences, Burapha University, Chonburi 20131, Thailand*
Niramon Thamwiriyasati − *Department of Medical Technology, Faculty of Allied Health Science, Burapha University, Chonburi 20131, Thailand*
Sanita Singsanan − *Department of Medical Technology, Faculty of Allied Health Science, Burapha University, Chonburi 20131, Thailand*

Complete contact information is available at: https://pubs.acs.org/10.1021/acsomega.4c02910

Notes

The authors declare no competing financial interest.

■ ACKNOWLEDGMENTS

This research was financially supported by the Thailand Science Research and Innovation, Fundamental Fund (FF2565, 211/2565) and the Faculty of Allied Health Sciences, Burapha University.

■ REFERENCES

(1) Socci, M. C.; Rodríguez, G.; Oliva, E.; Fushimi, S.; Takabatake, K.; Nagatsuka, H.; Felice, C. J.; Rodríguez, A. P. Polymeric Materials, Advances and Applications in Tissue Engineering: A Review. *Bioengineering* **2023**, *10*, 218.
(2) Anand, M.; Bhagania, M.; Kaur, K. Tissue engineering in plastic and reconstructive surgery: fostering advances in the 21st century via an understanding of the present state of the art and future possibilities. *Arch. Aesthetic Plast. Surg.* **2023**, *29*, 64−75.
(3) Chen, J.; Fan, Y.; Dong, G.; Zhou, H.; Du, R.; Tang, X.; Ying, Y.; Li, J. Designing biomimetic scaffolds for skin tissue engineering. *Biomater. Sci.* **2023**, *11*, 3051−3076.
(4) Giron, J.; Kerstner, E.; Medeiros, T.; Oliveira, L.; Machado, G.M.; Malfatti, C.F.; Pranke, P. Biomaterials for bone regeneration: an orthopedic and dentistry overview. *Braz. J. Med. Biol. Res.* **2021**, *54*, No. e11055.
(5) Krishani, M.; Shin, W. Y.; Suhaimi, H.; Sambudi, N. S. Development of Scaffolds from Bio-Based Natural Materials for Tissue Regeneration Applications: A Review. *Gels* **2023**, *9*, 100.
(6) Somaiah, C.; Kumar, A.; Mawrie, D.; Sharma, A.; Patil, S. D.; Bhattacharyya, J.; Swaminathan, R.; Jaganathan, B. G. Collagen Promotes Higher Adhesion, Survival and Proliferation of Mesenchymal Stem Cells. *PLoS One.* **2015**, *10*, No. e0145068.
(7) Manferdini, C.; Gabusi, E.; Sartore, L.; Dey, K.; Agnelli, S.; Almici, C.; Bianchetti, A.; Zini, N.; Russo, D.; Re, F.; Mariani, E.; Lisignoli, G. Chitosan-based scaffold counteracts hypertrophic and fibrotic markers in chondrogenic differentiated mesenchymal stromal cells. *J. Tissue Eng. Regener. Med.* **2019**, *13*, 1896−911.
(8) Jaipaew, J.; Wangkulangkul, P.; Meesane, J.; Raungrut, P.; Puttawibul, P. Mimicked cartilage scaffolds of silk fibroin/hyaluronic acid with stem cells for osteoarthritis surgery: Morphological, mechanical, and physical clues. *Mater. Sci. Eng., C* **2016**, *64*, 173−182.
(9) Vafa, E.; Bazargan-Lari, R.; Bahrololoom, M. E.; Amani, A. M. Effect of polyvinyl alcohol concentration on biomedical application of chitosan/bioactive glass composite coated on AZ91D magnesium alloy. *Mater. Chem. Phys.* **2022**, *291*, 126650.
(10) Kaviani, A.; Zebarjad, S. M.; Javadpour, S.; Ayatollahi, M.; Bazargan-Lari, R. Fabrication and characterization of low-cost freeze-gelated chitosan/collagen/ hydroxyapatite hydrogel nanocomposite scaffold. *Int. J. Polym. Anal. Charact.* **2019**, *24*, 191−203.
(11) Heidari, F.; Razavi, M.; Bahrololoom, M. E.; Bazargan-Lari, R.; Vashaee, D.; Kotturi, H.; Tayebi, L. Mechanical properties of natural chitosan/hydroxyapatite/magnetite nanocomposites for tissue engineering applications. *Mater. Sci. Eng., C* **2016**, *65*, 338−344.
(12) Stokols, S.; Tuszynski, M. H. Freeze-dried agarose scaffolds with uniaxial channels stimulate and guide linear axonal growth following spinal cord injury. *Biomaterials.* **2006**, *27*, 443−51.
(13) Ng, K. W.; Wang, C. C.; Mauck, R. L.; Kelly, T. A.; Chahine, N. O.; Costa, K. D.; Ateshian, G. A.; Hung, C. T. A layered agarose approach to fabricate depth-dependent inhomogeneity in chondrocyte-seeded constructs. *J. Orthop. Res.* **2005**, *23*, 134−141.
(14) Buschmann, M. D.; Gluzband, Y. A.; Grodzinsky, A. J.; Hunziker, E. B. Mechanical compression modulates matrix biosynthesis in chondrocyte/agarose culture. *J. Cell. Sci.* **1995**, *108*, 1497−1508.
(15) Kathuria, N.; Tripathi, A.; Kar, K. K.; Kumar, A. Synthesis and characterization of elastic and macroporous chitosan-gelatin cryogels for tissue engineering. *Acta Biomater.* **2009**, *5*, 406−418.
(16) Ratanavaraporn, J.; Damrongsakkul, S.; Sanchavanakit, N.; Banaprasert, T.; Kanokpanont, S. Comparison of gelatin and collagen scaffolds for fibroblast cell culture. *J. Met.: Mater. Miner.* **2017**, *16*, 31−36.
(17) Zhang, S.; Chen, L.; Jiang, Y.; Cai, Y.; Xu, G.; Tong, T.; Zhang, W.; Wang, L.; Ji, J.; Shi, P.; Ouyang, H. W. Bi-layer collagen/microporous electrospun nanofiber scaffold improves the osteochondral regeneration. *Acta Biomater.* **2013**, *9*, 7236−7247.
(18) Tamaddon, M.; Burrows, M.; Ferreira, S. A.; Dazzi, F.; Apperley, J. F.; Bradshaw, A.; Brand, D. D.; Czernuszka, J.; Gentleman, E. Monomeric, porous type II collagen scaffolds promote chondrogenic differentiation of human bone marrow mesenchymal stem cells in vitro. *Sci. Rep.* **2017**, *7*, 43519.
(19) Bhat, S.; Tripathi, A.; Kumar, A. Supermacroprous chitosan-agarose-gelatin cryogels: in vitro characterization and in vivo assessment for cartilage tissue engineering. *J. R Soc., Interface* **2011**, *8*, 540−554.
(20) Coenen, J.; Bernaerts, K. V.; Harings, W.; Jockenhoevel, S.; Ghazanfari, S. Elastic materials for tissue engineering applications: Natural, synthetic, and hybrid polymers. *Acta Biomater.* **2018**, *79*, 60−82.
(21) Bonani, W.; Singhatanadgige, W.; Pornanong, A.; Motta, A. Natural origin materials for osteochondral tissue engineering. *Adv. Exp. Med. Biol.* **2018**, *1058*, 3−30.
(22) Zhao, R.; Xu, Z.; Li, B.; Chen, T.; Mei, N.; Wang, C.; Zhou, Z.; You, L.; Wu, C.; Wang, X.; et al. A comparative study on agarose acetate and PDLLA scaffold for rabbit femur defect regeneration. *Biomed Mater.* **2019**, *14*, No. 065007.
(23) Meinel, L.; Hofmann, S.; Karageorgiou, V.; Kirker-Head, C.; McCool, J.; Gronowicz, G.; Zichner, L.; Langer, R.; Vunjak-Novakovic, G.; et al. The inflammatory responses to silk films in vitro and in vivo. *Biomater.* **2005**, *26*, 147−155.
(24) Shoulders, M. D.; Raines, R. T. Collagen structure and stability. *Annu. Rev. Biochem.* **2009**, *78*, 929−58.
(25) Farrell, E.; O'Brien, F. J.; Doyle, P.; Fischer, J.; Yannas, I.; Harley, B. A.; O'Connell, B.; Prendergast, P. J.; Campbell, V. A. A collagen-glycosaminoglycan scaffold supports adult rat mesenchymal stem cell differentiation along osteogenic and chondrogenic routes. *Tissue engineering.* **2006**, *12*, 459−68.
(26) Younesi, M.; Goldberg, V. M.; Akkus, O. A micro-architecturally biomimetic collagen template for mesenchymal condensation based cartilage regeneration. *Acta biomater.* **2016**, *30*, 212−221.
(27) Lien, S. M.; Ko, L. Y.; Huang, T. J. Effect of pore size on ECM secretion and cell growth in gelatin scaffold for articular cartilage tissue engineering. *Acta Biomater.* **2009**, *5*, 670−9.
(28) Chang, Y. H.; Wu, K. C.; Wang, C. C.; Ding, D. C. Enhanced chondrogenesis of human umbilical cord mesenchymal stem cells in a gelatin honeycomb scaffold. *J. Biomed Mater. Res. A* **2020**, *108*, 2069−79.
(29) Huang, Y.; Onyeri, S.; Siewe, M.; Moshfeghian, A.; Madihally, S. V. In vitro characterization of chitosan-gelatin scaffolds for tissue engineering. *Biomaterials.* **2005**, *26*, 7616−27.
(30) Gentile, P.; Nandagiri, V. K.; Daly, J.; Chiono, V.; Mattu, C.; Tonda-Turo, C.; Ciardelli, G.; Ramtoola, Z. Localised controlled

release of simvastatin from porous chitosan-gelatin scaffolds engrafted with simvastatin loaded PLGA-microparticles for bone tissue engineering application. *Mater. Sci. Eng. C Mater. Biol. Appl.* **2016**, *59*, 249−57.
(31) Su, K.; Wang, C. Recent advances in the use of gelatin in biomedical research. *Biotechnol. Lett.* **2015**, *37*, 2139−45.
(32) Song, J. H.; Kim, H. E.; Kim, H. W. Production of electrospun gelatin nanofiber by water-based co-solvent approach. *J. Mater. Sci. Mater. Med.* **2008**, *19*, 95−102.
(33) Lewandowska, K.; Sionkowska, A.; Grabska, S. Chitosan blends containing hyaluronic acid and collagen. Compatibility behaviour. *J. Mol. Liq.* **2015**, *212*, 879−884.
(34) Badhe, R. V.; Bijukumar, D.; Chejara, D. R.; Mabrouk, M.; Choonara, Y. E.; Kumar, P.; du Toit, L. C.; Kondiah, P. P. D.; Pillay, V. A composite chitosan-gelatin bi-layered, biomimetic macroporous scaffold for blood vessel tissue engineering. *Carbohydr. Polym.* **2017**, *157*, 1215−25.
(35) Liu, M.; Zheng, H.; Chen, J.; Li, S.; Huang, J.; Zhou, C. Chitosan-chitin nanocrystal composite scaffolds for tissue engineering. *Carbohydr. Polym.* **2016**, *152*, 832−40.
(36) Merlin Rajesh Lal, L. P.; Suraishkumar, G. K.; Nair, P. D. Chitosan-agarose scaffolds supports chondrogenesis of Human Wharton's Jelly mesenchymal stem cells. *J. Biomed Mater. Res. A* **2017**, *105*, 1845−55.
(37) Pooladi, A.; Bazargan-Lari, R. Adsorption of zinc and copper ions simultaneously on a low cost natural chitosan/hydroxyapatite/snail shell/nano magnetite composite. *Cellulose.* **2023**, *30*, 5687−5705.
(38) Bambaeero, A.; Bazargan-Lari, R. Simultaneous removal of copper and zinc ions by low cost natural Snail shell/hydroxyapatite/chitosan composite. *Chin. J. Chem. Eng.* **2021**, *33*, 221−230.
(39) Pooladi, A.; Bazargan-Lari, R. Simultaneous removal of copper and zinc ions by Chitosan/Hydroxyapatite/Nano-Magnetite composite. *J. Mater. Res. Technol.* **2020**, *9*, 14841−14852.
(40) Bazargan-Lari, R.; Zafarani, H. R.; Bahrololoom, M. E.; Nemati, A. Removal of Cu(II) ions from aqueous solutions by low-cost Natural hydroxyapatite/chitosan composite: Equilibrium, kinetic and thermodynamic studies. *J. Taiwan Inst. Chem. Eng.* **2014**, *45*, 1642−1648.
(41) Li, S. W.; He, H.; Zeng, R. J.; Sheng, G. P. Chitin degradation and electricity generation by Aeromonas hydrophila in microbial fuel cells. *Chemosphere.* **2017**, *168*, 293−299.
(42) Venkatesan, J.; Bhatnagar, I.; Kim, S. K. Chitosan-alginate biocomposite containing fucoidan for bone tissue engineering. *Mar. Drugs.* **2014**, *12*, 300−316.
(43) Shin, S. Y.; Park, H. N.; Kim, K. H.; Lee, M. H.; Choi, Y. S.; Park, Y. J.; Lee, Y. M.; Ku, Y.; Rhyu, I. C.; Han, S. B.; Lee, S. J.; Chung, C. P. Biological evaluation of chitosan nanofiber membrane for guided bone regeneration. *J. Periodontol.* **2005**, *76*, 1778−1784.
(44) Seol, Y. J.; Lee, J. Y.; Park, Y. J.; Lee, Y. M.; Young-Ku; Rhyu, I. C.; Lee, S. J.; Han, S. B.; Chung, C. P. Chitosan sponges as tissue engineering scaffolds for bone formation. *Biotechnol. Lett.* **2004**, *26*, 1037−1041.
(45) Muzzarelli, R. A.; Mattioli-Belmonte, M.; Tietz, C.; Biagini, R.; Ferioli, G.; Brunelli, M. A.; Fini, M.; Giardino, R.; Ilari, P.; Biagini, G. Stimulatory effect on bone formation exerted by a modified chitosan. *Biomaterials.* **1994**, *15*, 1075−1081.
(46) Zhou, D.; Qi, C.; Chen, Y. X.; Zhu, Y. J.; Sun, T. W.; Chen, F.; Zhang, C. Q. Comparative study of porous hydroxyapatite/chitosan and whitlockite/chitosan scaffolds for bone regeneration in calvarial defects. *Int. J. Nanomed.* **2017**, *12*, 2673−2687.
(47) Saravanan, S.; Leena, R. S.; Selvamurugan, N. Chitosan based biocomposite scaffolds for bone tissue engineering. *Int. J. Biol. Macromol.* **2016**, *93*, 1354−1365.
(48) Preethi Soundarya, S.; Haritha Menon, A.; Viji Chandran, S.; Selvamurugan, N. Bone tissue engineering: Scaffold preparation using chitosan and other biomaterials with different design and fabrication techniques. *Int. J. Biol. Macromol.* **2018**, *119*, 1228−1239.
(49) Lavanya, K.; Chandran, S. V.; Balagangadharan, K.; Selvamurugan, N. Temperature- and pH-responsive chitosan-based injectable hydrogels for bone tissue engineering. *Mater. Sci. Eng., C* **2020**, *111*, 110862.
(50) Ocloo, F. C. K.; Quayson, E. T.; Adu-Gyamfi, A.; Quarcoo, E. A.; Asare, D.; Serfor-Armah, Y.; Woode, B. K. Physicochemical and functional characteristics of radiation-processed shrimp chitosan. *Radiat. Phys. Chem.* **2011**, *80*, 837−841.
(51) Kumari, S.; Kumar Annamareddy, S. H.; Abanti, S.; Kumar Rath, P. Physicochemical properties and characterization of chitosan synthesized from fish scales, crab and shrimp shells. *Int. J. Biol. Macromol.* **2017**, *104*, 1697−1705.
(52) Begum, S.; Ikejima, K.; Ara, H.; Islam, M. Z. Solar Drying as an Option for Shrimp Processing Biowaste in Khulna District-Southwest Bangladesh. *J. Appl. Sci.* **2006**, *6*, 1302−1306.
(53) Yadav, M.; Goswami, P.; Paritosh, K.; Kumar, M.; Pareek, N.; Vivekanand, V. Seafood waste: a source for preparation of commercially employable chitin/chitosan materials. *Bioresour. Bioprocess.* **2019**, *6*, 8.
(54) Benjakul, S.; Sophanodora, P. Production of chitosan from banana prawn shell. *Songklanakarin J. Sci. Technol.* **1990**, *12*, 439−443.
(55) Lamarque, G.; Lucas, J.-M.; Viton, C.; Domard, A. Physicochemical Behavior of Homogeneous Series of Acetylated Chitosans in Aqueous Solution: Role of Various Structural Parameters. *Biomacromolecules.* **2005**, *6*, 131−142.
(56) Dutta, J.; Priyanka. A facile approach for the determination of degree of deacetylation of chitosan using acid-base titration. *Heliyon.* **2022**, *8*, No. e09924.
(57) Tripathi, A.; Melo, J. S. Preparation of a sponge-like biocomposite agarose−chitosan scaffold with primary hepatocytes for establishing an in vitro 3D liver tissue model. *ASC Adv.* **2015**, *5*, 30701−30710.
(58) Yan, L. P.; Wang, Y. J.; Ren, L.; Wu, G.; Caridade, S. G.; Fan, J. B.; Wang, L. Y.; Ji, P. H.; Oliveira, J. M.; Oliveira, J. T.; et al. Genipin-cross-linked collagen/chitosan biomimetic scaffolds for articular cartilage tissue engineering applications. *J. Biomed. Mater. Res.* **2010**, *95A*, 465−475.
(59) Chonanant, C.; Jearanaikoon, N.; Leelayuwat, C.; Limpaiboon, T.; Tobin, M. J.; Jearanaikoon, P.; Heraud, P. Characterisation of chondrogenic differentiation of human mesenchymal stem cells using synchrotron FTIR microspectroscopy. *Analyst* **2011**, *136*, 2542−2551.
(60) Nawar Tamzi, N.; Faisal, M.; Sultana, T.; Kumar Ghosh, S. Extraction and Properties Evaluation of Chitin and Chitosan Prepared from Different Crustacean Waste. *Bangladesh J. Vet. Anim. Sci.* **2020**, *8*, 69−76.
(61) Dash, M.; Chiellini, F.; Fernandez, E. G.; Piras, A. M.; Chiellini, E. Statistical approach to the spectroscopic determination of the deacetylation degree of chitins and chitosans. *Carbohydr. Polym.* **2011**, *86*, 65−71.
(62) Puvvada, Y.; Vankayalapati, S.; Sukhavasi, S. Extraction of chitin and chitosan from exoskeleton of shrimp for application in the pharmaceutical industry. *Int. Curr. Pharm. J.* **2012**, *1*, 258.
(63) Hussain, R.; Iman, M.; Maji, T. Determination of degree of deacetylation of chitosan and their effect on the release behavior of essential oil from chitosan and chitosan-gelatin complex microcapsules. *Int. J. Adv. Eng. Appl.* **2013**, *1*, 4−12.
(64) Pareek, N.; Vivekanand, V.; Agarwal, P.; Saroj, S.; Singh, R. P. Bioconversion to chitosan: a two stage process employing chitin deacetylase from Penicillium oxalicum SAEM-51. *Carbohydr. Polym.* **2013**, *96*, 417−425.
(65) Younes, I.; Hajji, S.; Frachet, V.; Rinaudo, M.; Jellouli, K.; Nasri, M. Chitin extraction from shrimp shell using enzymatic treatment. Antitumor, antioxidant and antimicrobial activities of chitosan. *Int. J. Biol. Macromol.* **2014**, *69*, 489−498.
(66) Hossain, M. S.; Iqbal, A. Production and characterization of Chitosan from shrimp waste. *J. Bangladesh Agril. Univ.* **2015**, *12*, 153−160.

https://doi.org/10.1021/acsomega.4c02910
ACS Omega 2024, 9, 39419−39429

(67) Mathaba, M. M.; Daramola, O. Effect of Chitosan's Degree of Deacetylation on the Performance of PES Membrane Infused with Chitosan during AMD Treatment. *Membranes.* **2020**, *10*, 52.
(68) Kumari, S.; Rath, P.; Sri Hari Kumar, A.; Tiwari, T. N. Extraction and characterization of chitin and chitosan from fishery waste by chemical method. *Environ. Technol. Innovation* **2015**, *3*, 77−85.
(69) Muñoz, G.; Valencia, C.; Valderruten, N.; Ruiz-Durántez, E.; Zuluaga, F. Extraction of chitosan from Aspergillus niger mycelium and synthesis of hydrogels for controlled release of betahistine. *React. Funct. Polym.* **2015**, *91*−*92*, 1−10.
(70) Hassan, A. I. Utilization of Waste: Extraction and Characterization of Chitosan from Shrimp Byproducts. *Civil. Environ. Res.* **2016**, *8*, 117−123.
(71) Rahman, M. M.; Maniruzzaman, M. A new route of production of the meso-porous chitosan with well-organized honeycomb surface microstructure from shrimp waste without destroying the original structure of native shells: Extraction, modification and characterization study. *Results Eng.* **2023**, *19*, 101362.
(72) Eddya, M.; Tbib, B.; El-Hami, K. A comparison of chitosan properties after extraction from shrimp shells by diluted and concentrated acids. *Heliyon.* **2020**, *6*, No. e03486.
(73) Hao, G.; Hu, Y.; Shi, L.; Chen, J.; Cui, A.; Weng, W.; Osako, K. Physicochemical characteristics of chitosan from swimming crab (Portunus trituberculatus) shells prepared by subcritical water pretreatment. *Sci. Rep.* **2021**, *11*, 1646.
(74) Zhang, Y.; Xue, C.; Xue, Y.; Gao, R.; Zhang, X. Determination of the degree of deacetylation of chitin and chitosan by X-ray powder diffraction. *Carbohydr. Res.* **2005**, *340*, 1914−1917.
(75) Mahboudi, S.; Pezeshki-Modaress, M.; Noghabi, K. A. The Study of Fibroblast Cell Growth on the Porous Scaffold of Gelatin−Starch Blend Using the Salt-Leaching and Lyophilization Method. *Int. J. Polym. Mater. Polym. Biomater.* **2015**, *64*, 653−659.
(76) Radhika Rajasree, S. R.; Gobalakrishnan, M.; Aranganathan, L.; Karthih, M. G. Fabrication and characterization of chitosan based collagen/ gelatin composite scaffolds from big eye snapper Priacanthus hamrur skin for antimicrobial and anti oxidant applications. *Mater. Sci. Eng., C* **2020**, *107*, 110270.
(77) Ribas, R. G.; Montanheiro, T. L. A.; Montagna, L. S.; Prado, R. F.; Lemes, A. P.; Bastos Campos, T. M.; Thim, G. P. Water Uptake in PHBV/Wollastonite Scaffolds: A Kinetics Study. *J. Compos. Sci.* **2019**, *3*, 74.
(78) Rahman, M.; Pervez, S.; Nesa, B.; Khan, M. A. Preparation and characterization of porous scaffold composite films by blending chitosan and gelatin solutions for skin tissue engineering. *Polym. Int.* **2013**, *62*, 79−86.
(79) Tagrida, M.; Nilsuwan, K.; Gulzar, S.; Prodpran, T.; Benjakul, S. Fish gelatin/chitosan blend films incorporated with betel (Piper betle L.) leaf ethanolic extracts: Characteristics, antioxidant and antimicrobial properties. *Food Hydrocolloids.* **2023**, *137*, 108316.
(80) Agarwal, T.; Narayan, R.; Maji, S.; Behera, S.; Kulanthaivel, S.; Maiti, T.; Banerjee, I.; Pal, K.; Giri, S. Gelatin/Carboxymethyl chitosan based scaffolds for dermal tissue engineering applications. *Int. J. Biol. Macromol.* **2016**, *93*, 1499−1506.
(81) Mozafari, M.; Kargozar, S.; de Santiago, G. T.; Mohammadi, M. R.; Milan, P. B.; Foroutan Koudehi, M.; Aghabarari, B.; Nourani, M. R. Synthesis and characterisation of highly interconnected porous poly(ε-caprolactone)-collagen scaffolds: a therapeutic design to facilitate tendon regeneration. *Mater. Technol.* **2018**, *33*, 29−37.
(82) Abbasi, N.; Hamlet, S.; Love, R. M.; Nguyen, N. T. Porous scaffolds for bone regeneration. *J. Sci.: Adv. Mater. Devices.* **2020**, *5*, 1−9.
(83) Cordell, J. M.; Vogl, M. L.; Wagoner Johnson, A. J. The influence of microporesize on the mechanical properties of bulk hydroxyapatite and hydroxyapatite scaffolds. *J. Mech. Behav. Biomed. Mater.* **2009**, *2*, 560−570.
(84) Felfel, R. M.; Gideon-Adeniyi, M. J.; Zakir Hossain, K. M.; Roberts, G. A.F.; Grant, D. M. Structural, mechanical and swelling characteristics of 3D scaffolds fromchitosan-agarose blends. *Carbohydr. Polym.* **2019**, *204*, 59−67.
(85) Han, Y.; Lian, M.; Wu, Q.; Qiao, Z.; Sun, B.; Dai, K. Effect of Pore Size on Cell Behavior Using Melt Electrowritten Scaffolds. *Front. Bioeng. Biotechnol.* **2021**, *9*, 629270.
(86) Nava, M. M.; Draghi, L.; Giordano, C.; Pietrabissa, R. The Effect of Scaffold Pore Size in Cartilage Tissue Engineering. *J. Appl. Biomater. Funct. Mater.* **2016**, *14*, e223−e229.
(87) Nehrer, S.; Breinan, H. A.; Ramappa, A.; Young, G.; Shortkroff, S.; Louie, L. K.; Sledge, C. B.; Yannas, I. V.; Spector, M. Matrix collagen type and pore size influence behaviour of seeded canine chondrocytes. *Biomaterials* **1997**, *18*, 769−776.
(88) Stenhamre, H.; Nannmark, U.; Lindahl, A.; Gatenholm, P.; Brittberg, M. Influence of pore size on the redifferentiation potential of human articular chondrocytes in poly(urethane urea) scaffolds. *J. Tissue Eng. Regener. Med.* **2011**, *5*, 578−588.

https://doi.org/10.1021/acsomega.4c02910
ACS Omega 2024, 9, 39419−39429